The Impact of Proton-Induced Activation on the Level of Radioactivity in D-^{3}He Fusion Reactors

H.Y. Khater and W.F. Vogelsang

October 1990

UWFDM-829

Presented at the 9th Topical Meeting on the Technology of Fusion Energy, 7–11 October 1990, Oak Brook IL.

FUSION TECHNOLOGY INSTITUTE

UNIVERSITY OF WISCONSIN

MADISON WISCONSIN

The Impact of Proton-Induced Activation on the Level of Radioactivity in D-^{3}He Fusion Reactors

H.Y. Khater and W.F. Vogelsang

Fusion Technology Institute
University of Wisconsin
1500 Engineering Drive
Madison, WI 53706

http://fti.neep.wisc.edu

October 1990

UWFDM-829

Presented at the 9th Topical Meeting on the Technology of Fusion Energy, 7–11 October 1990, Oak Brook IL.

THE IMPACT OF PROTON-INDUCED ACTIVATION ON THE LEVEL OF RADIOACTIVITY IN D-^{3}He FUSION REACTORS

H. Y. Khater and W. F. Vogelsang
Fusion Technology Institute
University of Wisconsin-Madison
1500 Johnson Drive
Madison, Wisconsin 53706-1687
(608) 262-8834

ABSTRACT

Experimental radionuclide production cross sections have been collected for protons with energy similar to those protons produced in a D-^{3}He fusion reactor. Proton energy-dependent cross sections (E_p < 14.7 MeV) were used along with the proton stopping data of Anderson and Ziegler to produce a proton-induced thick-target radionuclide activation yields library. In its present form, the library contains thick-target yield data for 164 radioactive isotopes. The library has been used in an activation analysis study aimed at investigating the effect of proton-induced activity on the total level of radioactivity generated in Apollo-L2 (a D-^{3}He tokamak fusion power reactor). Because protons have a short range in solid targets, their effect has been noticed only within the first wall of the reactor. Results showed that while neutron-induced specific activity generated in the reactor Tenelon first wall is 8.1×10^7 Ci/m^3, proton-induced specific activity only amounted to 6.37×10^5 Ci/m^3.

INTRODUCTION

One of the main goals in the design of fusion reactors is to achieve as clean an environment as possible. A D-^{3}He reactor has the potential to be an inherently safer fusion reactor due to the fact that most of the energy released in the plasma would be in the form of charged particles (protons) rather than neutrons. Most of the protons thermalize on the background plasma. Nevertheless, a small fraction of the protons would follow orbits which strike the reactor structure. A D-^{3}He tokamak reactor cannot afford to lose more than about five percent of its fast proton energy. When protons strike the first wall, nuclear reactions may be induced resulting in the production of radioactive isotopes.

Up to recently, activation analyses of D-^{3}He fusion reactors have been only focused on the radioactivity induced by neutrons produced from the D-D and D-T secondary reactions. Proton interaction with structural materials presents a potential source of induced radioactivity that has been ignored due to the general lack of cross section data for proton interaction with different target elements. A wide range of experimentally measured cross sections was used to produce a thick-target activation yields library for 164 radioactive isotopes. Even though most of the available cross sections for protons with energy < 14.7 MeV were those of (p,n) reactions, some cross sections for (p,γ), (p,2n), (p,α) and (p,pn) reactions were found and used in the calculations.

The library was used in this paper to calculate both the specific activity (Ci/m^3) and specific decay heat (MW/m^3) generated due to protons interacting with the first wall of a D-^{3}He tokamak reactor (Apollo-L2) that utilizes direct conversion.

THICK-TARGET YIELDS

The main difficulty in the application of protons for activation analysis is the need to use nuclear cross sections. The nuclear cross section is not a convenient quantity to use for this purpose because it is strongly dependent on proton energy, such that it continually varies as protons slow down in the irradiated material. Figure 1 shows the general features of a proton excitation function.[1] The excitation function gradually increases from the reaction threshold energy and reaches a maximum as the proton energy approaches the target coulomb barrier energy. As

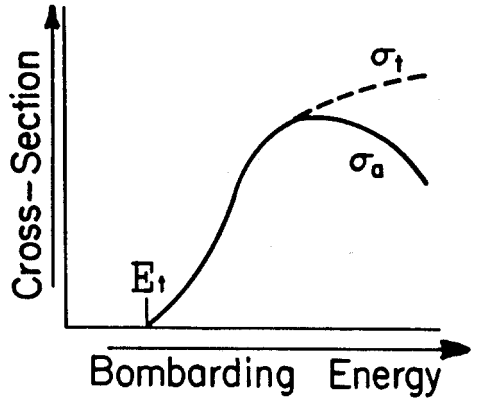

Figure 1. General features of proton excitation function.

shown in the figure, the cross section for a particular nuclear reaction (σ_a) starts to decrease as the probabilities of occurrence of other nuclear reactions increase. However, the total cross-section (σ_t) for all possible nuclear reactions continues to increase as proton energy increases. One alternative quantity to the cross section that is widely used is the thick-target yield "Y", which is usually expressed in the units of μCi/μA·hr.

An equation that describes the thick-target yield of a radioactive isotope produced from a stable nuclide can be written as:[2]

$$Y = 1.69 \times 10^8 \; n \lambda \int_0^{E_p} \frac{\sigma(E)}{S(E)} \, dE$$

where n(atoms/g) is the parent (stable) atom concentration, $\lambda(hr^{-1})$ is the radioisotope decay constant, E_p(MeV) is the proton energy, $\sigma(E)(cm^2)$ is the parent atom nuclear reaction cross section and $S(E)(MeV \cdot cm^2/g)$ is the parent atom stopping power.

Experimental cross section data were collected from several publications.[3,4,5] Data for protons (with energy <14.7 MeV) interacting with 109 naturally occurring isotopes of 58 target elements were found. For most nuclear reactions several sets of data were found for the same reaction, but not all of the cross sections covered the same proton energy range. In many instances significant differences existed in the measured cross section values for the same proton energy. In the absence of enough information about the measuring techniques that would indicate the level of accuracy associated with most of the cross section data, an averaging technique was adopted such that all available data can be taken into consideration. Several nuclear reactions lead to the formation of two different radioactive isotopes through the formation of two isomeric states. For such reactions where only the total cross section was given without having any other set of data for the same reaction that will help in estimating the branching ratio, a branching ratio of 50% was assumed.

The proton stopping powers were taken from the most complete data sets compiled by Anderson and Ziegler.[6] The authors used a mixture of experimentally and theoretically calculated proton stopping power values in compiling their report. At high proton energy, Anderson and Ziegler calculated the stopping power by using the Bethe equation:

$$S = \frac{4 \pi e^4 Z_1^2 Z_2}{mv^2} \left[\ln \left(\frac{2mv^2}{I} \right) + \ln \left(\frac{1}{1-\beta^2} \right) - \beta^2 - \frac{C}{Z_2} \right]$$

Here, e and m are the electronic charge and mass, respectively, Z_1 and Z_2 are the proton and target material atomic numbers, respectively, v is the proton velocity, $\beta = v/c$, where c is the speed of light, I is the effective ionization potential and C/Z_2 is the shell correction factor. The shell correction factor for all available experimental data for the proton stopping power was calculated by substituting for the theoretical value of the effective ionization potential in the Bethe equation. Several smooth curves of C/Z_2 as a function of E (energy expressed in keV/amu) were drawn for several elements. For those elements where C/Z_2 values were not smoothly varying as a function of Z_2, the authors altered the shape of some shell correction factor curves by using a power series formula that best fit the particular curve.

The proton stopping data were used with the measured cross sections to calculate the thick-target activation yields for 164 radionuclides. Thick-target radionuclide yields as a result of (p,n), (p,γ), (p,α), (p,2n) and (p,pn) reactions are shown in Tables 1, 2, 3, 4 and 5, respectively. E_{min} and E_{max} are the minimum and maximum energies (in MeV) for which the cross section data were found in the literature.

Table 1. Thick-target yields of radionuclides produced by p,n reactions

Target	E_{min}	E_{max}	Product	Y (μCi/μA·hr)
Li 7	1.88	5.50	Be 7	1.151E+02
Be 9	2.33	5.42	B 9	4.165E+26
B 10	4.94	11.70	C 10	3.710E+05
B 11	2.30	14.70	C 11	7.143E+05
C 13	3.24	5.27	N 13	5.268E+04
N 14	6.32	11.00	O 14	2.167E+06
N 15	3.72	14.70	O 15	3.124E+09
O 18	2.30	14.70	F 18	1.035E+05
F 19	4.21	4.93	Ne 19	2.264E+05
Na 23	4.85	11.60	Mg 23	1.092E+07
Mg 25	5.28	8.89	Al 25	1.348E+07
Mg 26	4.97	6.97	Al 26	1.338E-06
Mg 26	4.97	5.82	Al 26m	8.706E+05
Al 27	5.77	14.70	Si 27	5.258E+07
S 34	0.10	14.70	Cl 34m	8.315E+04
Cl 37	1.60	5.00	Ar 37	1.068E+01
K 41	1.11	5.96	Ca 41	1.408E-05
Sc 45	3.28	14.70	Ti 45	4.923E+04
Ti 47	4.00	14.00	V 47	2.142E+05
Ti 48	5.00	14.70	V 48	5.453E+02
Ti 49	1.30	6.00	V 49	3.075E+00
V 51	1.57	14.70	Cr 51	4.233E+02
Cr 52	5.80	14.70	Mn 52	4.541E+02
Cr 52	5.80	14.70	Mn 52m	3.153E+05
Cr 53	1.42	5.88	Mn 53	4.509E-07
Cr 54	2.22	9.00	Mn 54	1.175E+01
Mn 55	1.00	8.10	Fe 55	2.230E+00
Fe 56	4.80	14.70	Co 56	6.802E+01
Fe 57	1.60	14.00	Co 57	1.840E+01
Co 59	1.89	14.70	Ni 59	3.007E-04
Ni 60	6.70	14.70	Cu 60	2.441E+05
Ni 61	2.49	14.10	Cu 61	4.825E+04
Ni 62	4.82	14.70	Cu 62	1.023E+06
Ni 64	2.50	14.70	Cu 64	1.664E+04
Cu 63	3.80	14.70	Zn 63	2.478E+05

Table 1 (continued)

Target	E_{min}	E_{max}	Product	Y (μCi/μA·hr)
Cu 65	1.80	14.70	Zn 65	3.408E+01
Zn 64	8.10	11.90	Ga 64	6.993E+05
Zn 66	5.50	14.70	Ga 66	1.878E+04
Zn 67	1.85	6.37	Ga 67	1.948E+02
Zn 68	3.38	14.70	Ga 68	2.060E+05
Ga 69	3.00	14.70	Ge 69	6.579E+03
Ga 71	1.04	14.70	Ge 71	3.866E+02
Ga 71	1.04	14.70	Ge 71m	1.971E+10
Ge 74	3.42	5.83	As 74	1.025E+01
As 75	1.67	8.10	Se 75	1.131E+01
Se 77	2.18	14.70	Br 77	1.469E+03
Se 77	2.18	5.54	Br 77m	4.517E+04
Se 78	4.53	6.28	Br 78	5.477E+04
Se 80	2.67	6.39	Br 80	2.658E+04
Se 80	2.69	6.38	Br 80m	5.311E+02
Se 82	0.93	6.40	Br 82	3.394E+02
Br 79	3.00	14.70	Kr 79	4.965E+03
Rb 87	2.65	12.00	Sr 87m	1.645E+04
Sr 87	2.61	6.82	Y 87	1.064E+02
Sr 87	2.61	6.82	Y 87m	6.573E+02
Sr 88	4.80	14.70	Y 88	1.747E+03
Sr 88	4.80	14.70	Y 88m	3.864E+11
Y 89	3.55	14.70	Zr 89	1.369E+03
Y 89	3.66	14.70	Zr 89m	9.060E+05
Zr 90	7.00	14.70	Nb 90	3.560E+03
Zr 90	4.94	14.70	Nb 90m	1.266E+07
Zr 91	3.50	11.20	Nb 91m	3.883E+01
Zr 92	3.50	6.67	Nb 92	1.527E-09
Zr 92	3.50	9.00	Nb 92m	1.198E+02
Zr 96	2.73	9.00	Nb 96	1.767E+03
Nb 93	1.26	14.70	Mo 93	4.897E-03
Nb 93	1.26	14.70	Mo 93m	1.056E+03
Mo 94	6.00	9.00	Tc 94	4.457E+02
Mo 94	5.50	9.00	Tc 94m	2.129E+04
Mo 95	4.00	9.00	Tc 95	9.346E+02
Mo 95	4.00	9.00	Tc 95m	4.969E+00
Mo 96	10.00	14.70	Tc 96	6.866E+01
Mo 96	4.50	14.70	Tc 96m	1.452E+05
Mo 100	4.00	9.00	Tc 100	7.893E+06
Ru 100	4.25	6.19	Th 100	6.511E+01
Ru 100	4.25	6.19	Rh100m	1.745E+04
Ru 101	2.92	12.00	Rh101m	4.619E+02
Rh 103	2.31	10.00	Pd 103	1.046E+02
Pd 104	6.00	9.00	Ag 104	1.685E+03
Pd 104	6.00	9.00	Ag104m	3.912E+04
Pd 105	5.00	9.00	Ag 105	1.859E+01
Pd 105	4.00	9.00	Ag105m	5.588E+04
Pd 106	6.50	9.00	Ag 106	3.006E+04
Pd 106	6.00	9.00	Ag106m	1.103E+01
Pd 108	4.00	9.00	Ag 108	5.646E+05
Pd 110	2.11	9.00	Ag 110	3.374E+06
Pd 110	2.11	9.00	Ag110m	4.879E-01
Ag 107	1.90	14.70	Cd 107	1.853E+04
Ag 109	2.09	10.50	Cd 109	2.868E+00
Cd 110	4.50	14.70	In 110	9.810E+04
Cd 110	4.50	14.70	In110m	5.974E+03
Cd 111	1.50	14.70	In 111	1.090E+03
Cd 111	1.50	14.70	In111m	4.626E+05
Cd 112	3.14	14.70	In 112	3.183E+05
Cd 112	3.14	14.70	In112m	2.025E+05

Table 1 (continued)

Target	E_{min}	E_{max}	Product	Y (μCi/μA·hr)
Cd 113	4.70	14.70	In113m	1.648E+04
Cd 114	2.20	10.00	In 114	9.881E+05
Cd 114	2.20	14.70	In114m	3.986E+01
Cd 116	1.50	8.41	In 116	3.290E+06
Cd 116	1.50	14.70	In116m	2.188E+04
Sn 117	2.83	7.07	Sb 117	1.179E+03
Sn 118	4.53	6.92	Sb 118	4.691E+04
Sn 118	4.53	6.92	Sb118m	5.473E+02
Sn 119	2.62	7.08	Sb 119	9.395E+01
Sn 120	3.56	6.97	Sb 120	7.924E+03
Sn 120	3.68	6.97	Sb120m	1.158E+01
Sn 122	2.64	9.10	Sb 122	3.857E+02
Sn 122	2.64	9.10	Sb122m	5.858E+04
Sn 124	2.61	7.11	Sb 124	2.732E+00
Sb 121	5.20	9.00	Te 121	2.192E+01
Sb 121	5.20	9.00	Te121m	1.350E+00
Te 124	9.58	14.70	I 124	5.343E+02
Te 128	3.31	6.24	I 128	1.636E+03
Te 130	2.73	14.70	I 130	2.805E+03
Te 130	2.73	5.66	I 130m	9.982E+02
I 127	3.01	14.70	Xe 127	5.618E+01
I 127	3.01	14.70	Xe127m	2.454E+06
Ba 134	10.50	11.70	La 134	6.819E+03
La 139	4.50	10.30	Ce 139	3.836E+00
La 139	4.50	10.30	Ce139m	8.142E+05
Ce 142	3.80	14.70	Pr 142	7.114E+02
Ce 142	3.80	14.70	Pr142m	5.593E+04
Pr 141	4.84	14.70	Nd 141	3.622E+04
Pr 141	5.32	14.70	Nd141m	1.912E+06
Nd 148	9.00	14.70	Pm 148	4.318E+01
Nd 148	9.00	14.70	Pm148m	3.138E+00
Gd 160	4.30	14.70	Tb 160	5.873E+00
Tm 169	3.30	14.70	Yb 169	3.189E+01
Tm 169	3.30	14.70	Yb169m	1.916E+06
Hf 180	6.50	9.00	Ta180m	2.202E+02
Ta 181	4.50	14.70	W 181	3.655E+00
Au 197	7.00	14.70	Hg 197	9.733E+01
Au 197	7.00	14.70	Hg197m	2.632E+02
Pb 206	5.00	14.70	Bi 206	2.030E+02
Bi 209	2.90	14.70	Po 209	1.906E-02

Table 2. Thick-target yields of radionuclides produced by p,γ reactions

Target	E_{min}	E_{max}	Product	Y (μCi/μA·hr)
C 12	0.09	11.00	N 13	9.179E+03
Ca 42	0.69	5.43	Sc 43	8.665E+00
Ni 60	0.61	14.70	Cu 61	2.004E+02
Zn 64	1.47	11.00	Ga 65	1.151E+03
Se 82	6.85	14.70	Br 83	1.006E+02
Zr 90	1.97	5.70	Nb 91	1.262E-06
Zr 90	1.97	5.70	Nb 91m	7.434E-02
Mo 100	8.00	14.70	Tc 101	7.207E+02
Cd 114	3.00	8.00	In115m	4.906E+00
Sn 112	5.00	9.00	Sb 113	1.802E+04
Te 130	6.00	14.70	I 131	7.418E-01
Ce 142	5.50	14.70	Pr 143	2.778E-01
Bi 209	6.00	14.70	Po 210	2.292E-02

Table 3. Thick-target yields of radionuclides produced by p,α reactions

Target	E_{min}	E_{max}	Product	Y (μCi/μA·hr)
N 14	4.00	14.70	C 11	4.807E+05
O 16	6.22	14.70	N 13	1.664E+05
Ne 20	5.58	10.28	F 17	1.667E+06
Mg 24	9.22	13.75	Na 21	2.863E+06
Mg 25	5.00	14.70	Na 22	2.904E+00
Ni 58	7.40	14.70	Co 55	3.032E+02
Ni 60	6.80	14.70	Co 57	2.054E+00
Ni 61	7.00	14.40	Co 58	9.220E+00
Ni 61	7.00	14.40	Co 58m	1.722E+03
Zn 64	7.10	14.70	Cu 61	4.404E+03
Zr 90	12.00	14.70	Y 87	2.737E+00
Zr 90	12.00	14.70	Y 87m	1.691E+01
Sn 120	3.50	14.70	In117m	1.634E+01
Hg 202	12.00	14.70	Au 199	4.723E-02

Table 4. Thick-target yields of radionuclides produced by p,2n reactions

Target	E_{min}	E_{max}	Product	Y (μCi/μA·hr)
Cu 63	14.00	14.70	Zn 62	9.859E+00
Ga 69	13.10	14.70	Ge 68	3.278E+00
Y 89	13.30	14.70	Zr 88	1.617E+00
Cd 110	12.60	14.70	In 109	1.698E+03
Cd 110	12.80	14.70	In109m	6.538E+04
Cd 111	11.80	14.70	In 110	2.130E+04
Cd 111	11.20	14.70	In110m	8.493E+02
Cd 112	9.40	14.70	In 111	5.071E+02
Cd 112	10.80	14.70	In111m	9.079E+04
Te 124	12.20	14.70	I 123	9.103E+02
Pr 141	9.00	14.70	Nd 140	4.863E+02

Table 5. Thick-target yields of radionuclides produced by p,pn reactions

Target	E_{min}	E_{max}	Product	Y (μCi/μA·hr)
C 12	8.50	14.70	C 11	1.285E+04
Sc 45	11.30	14.70	Sc 44	2.467E+03
Sc 45	12.00	14.70	Sc 44m	1.029E+02
Co 59	12.00	14.70	Co 58	4.450E-01
Co 59	12.10	14.70	Co 58m	1.464E+02
Cu 63	14.00	14.70	Cu 62	5.984E+03
Cu 65	9.80	14.70	Cu 64	3.105E+02
Ga 69	13.90	14.70	Ga 68	2.094E+03
Br 81	10.00	14.70	Br 80	6.457E+03
Br 81	0.15	14.70	Br 80m	1.128E+03
Y 89	12.70	14.70	Y 88	7.672E-01
Y 89	12.70	14.70	Y 88m	9.814E+08
Ag 107	8.78	14.70	Ag 106	1.356E+03
Ag 107	11.00	14.70	Ag106m	8.894E+00
Cd 110	12.60	14.70	Cd 109	7.318E-02
Ta 181	13.40	14.70	Ta180m	4.874E+00
Au 197	10.00	14.70	Au 196	1.464E+00
Au 197	10.00	14.70	Au196m	2.235E+01

PROTON ACTIVATION ANALYSIS

A D-^{3}He fusion reactor is expected to be inherently safer than either D-T or D-D fueled reactors. Calculations of radioactivity induced by both neutrons and protons interacting with the structural materials are essential to have a real understanding of the safety problems that might be associated with such a reactor. The development of proton and general charged particle activation analysis has been slow due to the following reasons:

(1) The detailed excitation functions for charged particle reactions are only known for very few elements and most of the time they are hard to find at the desired energy.
(2) Charged particles have a limited penetration range in solids. There has been a general lack in the availability of reliable data for the range and the stopping power in all elements.
(3) The probability of occurrence of several nuclear reactions simultaneously at the same charged particle energy increases the possibility of nuclear interference.

In this paper, the proton-induced radioactivity has been calculated through the use of thick-target yields. The following assumptions were made:

(a) The parent atoms are stable such that the radioactive isotopes are only produced as products of nuclear interactions between protons and the target material.
(b) No chains are assumed (i.e., no removal of the radioactive isotopes by absorption).
(c) No regard to the reduction in the number of parent atoms.

From the definition of the thick-target yield "Y" of any radioactive isotope, the activity produced takes the form:

$$A = Y I \left(\frac{1 - e^{-\lambda t}}{\lambda}\right)$$

where I is the proton current in μA and t is the irradiation time in hours.

If a radioactive isotope "i" is produced as the result of a proton interacting with its parent nuclide "j" which in turn is contained as a homogeneous admixture to the irradiated structural material (first wall) "k", the activity produced is:

$$A^i_{jk} = Y_{jk} I \left(1 - e^{-\lambda_i t}\right)$$

as

$$Y_{jk} = Y \eta_{jk} F$$

where Y is the thick-target yield of the radioisotope "i" for a thick target consisting entirely of its parent nuclide "j", η_{jk} is the relative concentration (by weight) of the nuclide "j" in the first wall "k" and λ_i is the radioactive isotope "i" decay constant. F is a factor which takes into account the difference between the proton stopping power of the parent

nuclide "j" and of the irradiated alloy "k", and can be defined as:

$$F = \frac{R_k}{R_j} = \frac{1}{x_1 + x_2 \frac{R_1}{R_2} + x_3 \frac{R_1}{R_3} + \ldots}$$

Here, R_j is the range of protons in the parent nuclide "j", R_k is the range of protons in the irradiated alloy "k" and R_1, R_2, R_3, ... are the ranges of protons in the individual nuclides forming the irradiated alloy "k". x_1, x_2, x_3, ... are the weight proportions of the individual elements in the target compound.

If the radioisotope "i" is formed simultaneously from several stable nuclides in the first wall, the radioisotope activity can be written as:

$$A_k^i = I\,(1 - e^{-\lambda_i t}) \sum_n Y_{nk}$$

The index "n" refers to a parent nuclide in the first wall that produces the radioactive isotope through a nuclear reaction with the incident proton.

APOLLO-L2 ACTIVATION ANALYSIS

To examine the contribution of proton-induced activity to the total generated activity in advanced fuel fusion reactors, activation analysis was performed for Apollo-L2 which is a D-^{3}He fueled tokamak reactor that utilizes direct conversion. The reactor is operated for 30 full power years and produces a net electric power of 1200 MW_e; the peak neutron wall loadings on the inboard and outboard sides of the first wall midplane are 0.1 and 0.14 MW/m^2, respectively. Only 5% of the 14.7 MeV protons produced in the plasma are assumed to strike the reactor first wall. Since the level of induced radioactivity depends on the type of alloy used as a structural material, the comparison between the proton-induced and neutron-induced radioactivity was conducted for a first wall made of the low activation austenitic steel Tenelon. Results for the neutron-induced activity were taken from a previous paper.[7] The composition of the Tenelon used is that presented in the Blanket Comparison and Selection Study (BCSS) report .[8]

The calculations showed while proton-induced activity might add a very small contribution to the neutron-induced activity for short-term (<5 years) and mid-term (<10 years) activities after shutdown, its contribution to long-term activity is negligible if compared to the activity induced by neutrons in the reactor first wall. The short-term induced activity is dominated by ^{56}Mn($T_{1/2}$ = 2.6 hr), ^{54}Mn($T_{1/2}$ = 313 day), ^{55}Fe($T_{1/2}$ = 2.7 yr) and ^{51}Cr($T_{1/2}$ = 27.7 day) in the case of neutrons. In the case of proton-induced activity the major contributors are ^{56}Co($T_{1/2}$ = 78.5 day) produced from ^{56}Fe, ^{57}Co($T_{1/2}$ = 271 day) produced from ^{57}Fe and ^{60}Ni, ^{52}Mn($T_{1/2}$ = 5.63 day) and ^{52m}Mn ($T_{1/2}$ = 21.4 min) produced from ^{52}Cr, ^{54}Mn produced from ^{54}Cr and ^{55}Fe produced from ^{55}Mn. While ^{57}Co is produced through (p,n) and (p,α) reactions, other contributors to the proton-induced activity are mainly produced through (p,n) reactions. In the period between 5 years and 10 years after shutdown, ^{55}Fe, ^{54}Mn, ^{63}Ni($T_{1/2}$ = 100 yr) and ^{60}Co($T_{1/2}$ = 5.27 yr) represent the major contributors to the neutron-induced activity. For the same period of time, proton-induced activity is dominated by ^{55}Fe, ^{57}Co and ^{54}Mn. The long-term activity is only due to radionuclides produced from neutron interaction with the reactor first wall such as ^{14}C($T_{1/2}$ = 5730 yr), ^{59}Ni($T_{1/2}$ = 80,000 yr) and ^{53}Mn($T_{1/2} = 3.8 \times 10^6$ yr). A comparison between proton and neutron induced specific activity as a function of time following shutdown is shown in Figure 2.

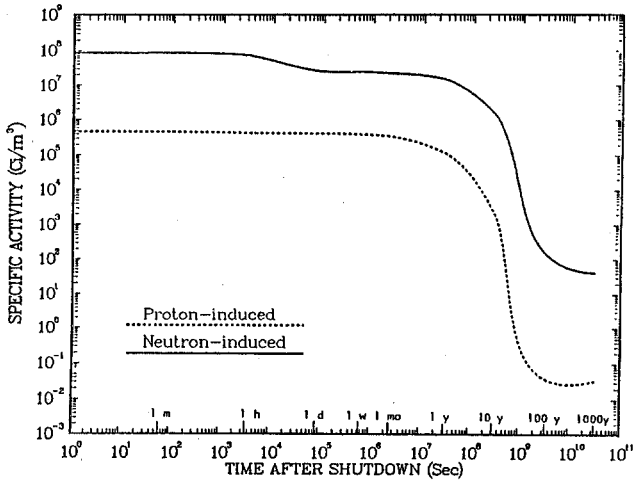

Figure 2. Comparison between proton and neutron induced specific activity in the first wall of Apollo-L2.

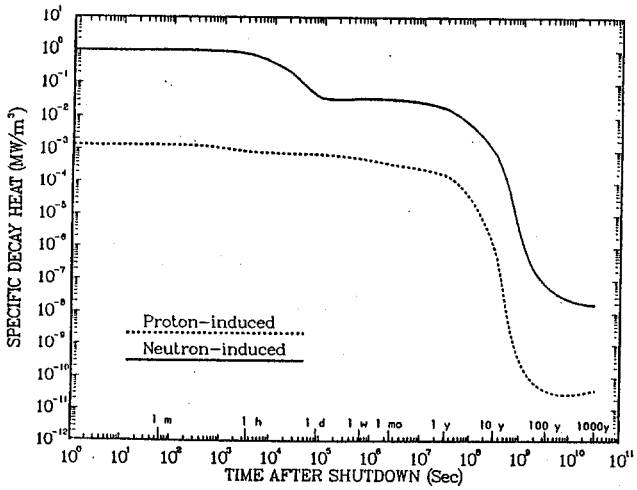

Figure 3. Comparison between the specific decay heat generated by protons and neutrons in the first wall of Apollo-L2.

The decay heat generated in the Apollo-L2 first wall is dominated by the same radionuclide that dominated the level of activity after shutdown. ^{56}Mn produced from neutron interaction with the Tenelon first wall produces 96% of the decay heat generated at shutdown. Proton-induced decay heat is mostly produced by ^{52}Mn and ^{52m}Mn. Figure 3 shows a comparison for the specific decay heat generated following shutdown. A high neutron-induced decay heat is generated in the first wall within the first eight hours following shutdown due to the high content of manganese in Tenelon. In the meanwhile, one can notice that proton-induced decay heat generated following shutdown can be neglected if compared to the neutron-induced one. Previous loss of coolant accident (LOCA) analysis for Apollo-L2 showed that the maximum first wall temperature two weeks after LOCA levels off close to 200°C. The proton-induced decay heat results show that the expected thermal response of the first wall following a loss of coolant accident would remain the same.

As shown in a previous paper an Apollo-L2 Tenelon structure would easily qualify as class C low level waste (LLW) and hence would meet the U.S. requirements for shallow land burial. Added contribution from long lived radioactive nuclides produced by proton interactions with the reactor structure will have no effect on the previous waste classification. The major contributors to the proton-induced activity in Apollo-L2 are those with half-lives less than 5 years. Hence, their contribution to the waste disposal rating (WDR) is negligible as the 10CFR61 limits[9] are given to radionuclides with half-lives greater than 5 years.

CONCLUSIONS

A library that contains thick-target activation yields for nuclides produced by proton activation of several stable nuclides has been compiled. Only experimental radionuclide production cross sections from the literature were used in the thick-target yield calculations. Thick-target yield values from the library were used to calculate the proton-induced activity in the first wall (Tenelon) of a D-^{3}He reactor Apollo-L2. The results showed that proton-induced activity represents a small fraction of the total radioactivity generated in the Tenelon structure. The inclusion of theoretically estimated values for the unknown radionuclide production excitation functions is not expected to change the conclusion that neutron-induced activity remains the only dominant source of radioactivity in D-^{3}He fusion reactors. The only other potential source of radioactivity that was not included in this study is the activity induced by neutrons produced from proton interaction with the reactor structural materials through (p,n) reactions. The radioactivity generated by these neutrons will be the topic of future study.

ACKNOWLEDGMENTS

This work was supported by the Wisconsin Electric Utilities Research Foundation, the Grainger Corporation, Fusion Power Associates, the Electric Power Research Institute, McDonnell Douglas Corporation and the Grumman Aerospace Corporation.

REFERENCES

1. R.S. TILBURY, "Activation Analysis with Charged Particles," NAS-NS-3110, National Academy of Sciences, National Research Council (1967).

2. N.N. KRASANOV, "Thick Target Yield," International Journal of Applied Radiation and Isotopes, 25, 223 (1974).

3. B.V. ROBOUCH and A. GENTILINI, "Proton-Nuclide Reaction Cross Sections, a Collection of Data from Literature," RT/FUS/87/31, Comitato Nazionale Per La Ricerca E Per Lo Sviluppo Dell'Energia Nucleare E Delle Energie Alternative (1987).

4. H. MÜNZEL et al., "Karlsruhe Charged Particle Reaction Data Compilation," Physics Data, No. 15, Fachinformationszentrum, Karlsruhe (1982).

5. NATIONAL NUCLEAR DATA CENTER, "On-Line Data Bases," Brookhaven National Laboratory.

6. H.H. ANDERSON and J.F. ZIEGLER, "Hydrogen Stopping Powers and Ranges in All Elements," Pergamon Press, New York (1977).

7. H.Y. KHATER, M.E. SAWAN, S.W. LOMPERSKI and I.N. SVIATOSLAVSKY, "Activation and Safety Analyses for the D-^{3}He Fueled Tokamak Reactor Apollo," Proceedings of the IEEE 13th Symposium on Fusion Engineering, 2-6 October 1989, Knoxville, TN, pp. 728-731 (1989).

8. D. SMITH et al., "Blanket Comparison and Selection Study," ANL/FPP/TM-122, Argonne National Laboratory, (1984).

9. NUCLEAR REGULATORY COMMISSION, 10CFR part 61, "Licensing Requirements for Land Disposal of Radioactive Waste," Federal Register, FR 47, 57446 (1982).